



Establishing the Safe Space via Physiologically Based Biopharmaceutics Modeling. Case Study: Fevipiprant/QAW039

Alexandros Kourentas¹ · Monika Gajewska² · Wen Lin^{3,4} · Sundeep S. Dhareshwar⁵ · Caroline Steib-Lauer⁶ · Swarupa Kulkarni³ · Stefan Hirsch⁷ · Tycho Heimbach^{3,8} · Martin Mueller-Zsigmondy¹

Received: 11 November 2022 / Accepted: 20 January 2023 / Published online: 14 February 2023
© The Author(s), under exclusive licence to American Association of Pharmaceutical Scientists 2023

Abstract

Physiologically based pharmacokinetic and absorption modeling has increasingly been implemented for biopharmaceutics applications to define the safe space for drug product quality attributes such as dissolution. For fevipiprant/QAW039, simulations were performed to assess the impact of *in vitro* dissolution on the *in vivo* performance of immediate-release film-coated tablets during development and scaling up to commercial scale. A fevipiprant dissolution safe space was established using observed clinical intravenous and oral PK data from bioequivalent and non-bioequivalent formulations. Quality control dissolution profiles with tablets were used as GastroPlus™ model inputs to estimate the *in vivo* dissolution in the gastrointestinal tract and to simulate human exposure. The model was used to evaluate the intraluminal performance of the dosage forms and to predict the absorption rate limits for the 450 mg dose. The predictive model performance was demonstrated for various oral dosage forms (150–500 mg), including the non-bioequivalent batches in fasted healthy adults. To define the safe space at 450 mg, simulations were performed using theoretical dissolution profiles. A specification of Q = 80% dissolved in 60 min or less for an immediate-release oral solid dosage form reflected the boundaries of the safe space. The dissolution profile of the 450 mg commercial scale batch was within a dissolution region where bioequivalence is anticipated, not near an edge of failure for dissolution, providing additional confidence to the proposed acceptance criteria. Thus, the safe space allowed for a wider than 10% dissolution difference for bioequivalent batches, superseding f_2 similarity analyses.

Keywords fevipiprant · GastroPlus™ · PBBM · safe space · twin-screw melt granulation

Introduction

The need to translate the knowledge gained from various *in vitro* dissolution studies to the *in vivo* performance of a dosage form has increased the number of *in silico* models developed using various commercially available software (1–3).

Their usefulness as a biopharmaceutics tool stems from their ability to predict the impact of many formulation factors that can influence oral drug absorption, including properties of the active pharmaceutical ingredient (API) and dosage form as well as the dynamic environment of the gastrointestinal (GI) tract on the resulting plasma pharmacokinetic (PK)

✉ Martin Mueller-Zsigmondy
martin.mueller-zsigmondy@novartis.com

¹ Dissolution & Biopharmaceutics, Analytical Research and Development, Technical Research and Development, Novartis AG, CH-4056 Basel, Switzerland

² Pharmacokinetics Sciences, Translational Medicine, Novartis Institutes for BioMedical Research, Novartis AG, CH-4056 Basel, Switzerland

³ Pharmacokinetics Sciences, Translational Medicine, Novartis Institutes for BioMedical Research, Novartis Pharmaceuticals Corporation, New Jersey, One Health Plaza, East Hanover 07936, USA

⁴ Present Address: PK/PD Group, Pharmacokinetics, Dynamics and Metabolism, Sanofi, Bridgewater, NJ, USA

⁵ Global Program Management, Global Drug Development, Novartis Pharmaceuticals Corporation, East Hanover, NJ 07936, USA

⁶ Analytical Research and Development, Technical Research and Development, Novartis AG, CH-4056 Basel, Switzerland

⁷ Global Drug Development, Technical Portfolio and Project Management, Technical Research and Development, Novartis AG, CH-4056 Basel, Switzerland

⁸ Present Address: Sterile and Specialty Products, Biopharmaceutics, Merck & Co., Inc., Rahway, NJ 07065, USA

profile. In this way, the tools can integrate *in vitro* measurements of properties such as solubility, permeability, and dissolution performance to build an overall picture of the biopharmaceutics risk.

The applications of physiologically based biopharmaceutics modeling (PBBM) to support drug product quality have been highlighted by regulators and the industry (4, 5). Such applications include the safe space design, which has been defined as the boundaries demarcated by *in vitro* specifications (i.e., dissolution or when applicable other relevant drug product quality attributes), within which drug product variants are anticipated to be bioequivalent (BE) to one another (6). The utilization of safe space leads to the justification of clinically relevant dissolution specifications (CRDS). These specifications may, in turn, reduce the number of clinical studies needed to support manufacturing processes or site changes and provide an opportunity for accelerating drug product development.

While the safe space approach is well recognized by Health Authorities (7), relatively few PBBM cases supporting drug product quality are reported in the literature. For instance, Pepin *et al.* developed a virtual drug substance batch for lesinurad with a particle size distribution at the limit of the proposed specification for particle size. Based on these simulations, such a batch was anticipated to be bioequivalent to a clinical reference (8). In addition, Loisios *et al.* showed that based on a derived safe space for naproxen, *in vitro* dissolution rate is not critical for the clinical performance of naproxen products (9). As a result, naproxen could be eligible for BCS-based biowaivers based on *in vitro* dissolution measured under intestinal conditions. Furthermore, Heimbach *et al.* reported five cases using PBBM to establish a safe space for BCS II and IV across different companies. Following model development and verification, the implementation of safe space was used for internal decision-making when considering regulatory requirements (10). Finally, a more recent example of safe space was reported by Laisney *et al.*, where PBBM was used to support the formulation development of ribociclib, an orally bioavailable selective CDK4/6 inhibitor. Ribociclib, a weak base with moderate permeability, can be dissolved completely at the normal acidic stomach pH *in vitro*. Virtual trial simulations for virtual batches with slower dissolution were used to define a safe space for tablets, where bioequivalence (BE) is expected (11).

Fevipirant/QAW039 is a novel oral prostaglandin D2 receptor 2 (DP2; also known as CRTh2) antagonist that was clinically advanced for the treatment of chronic asthma (12). To explore the formulation design/knowledge space and eventually to scale up the twin-screw melt granulation (TSMG)-based process for commercial readiness, pilot-scale prototype tablets were melt-granulated with different extruder screw configurations designed to vary the extent

of granulation, which in turn resulted in different dissolution profiles. A BE study, specifically at the highest dose of 450 mg with the “fast” and “slow” dissolving prototype tablets, was led to non-bioequivalence primarily due to the lower geometric mean ratio of C_{max} . Given the primary objective was delineating the release profiles for the prototype tablets, these sets of data provided an opportunity to develop a safe space for fevipirant using PBBM in Gastro-Plus™. This article describes the work performed and the modeling strategy applied, which was used for setting up CRDS for the 450 mg dose, supporting drug product quality.

Materials and Methods

Film-coated Tablet Batches used in the PBBM Application

Fevipirant is a zwitterionic, low molecular weight, BCS class IV drug substance. Two weight proportional immediate-release film-coated tablets of 150 mg and 450 mg were formulated using a twin-screw melt granulation (TSMG) as the primary unit operation. Formulation development at pilot scale was performed using a 27 mm (ZSE-27) while scale up to commercial scale was performed using a 50 mm (ZSE-50) co-rotating, intermeshing, twin-screw extruders (Leistritz Extrusionstechnik GmbH, Germany) (13). The formulation design space to optimize the melt granulation process parameters, and related tablet dissolution performance, was explored using pilot scale “fast” and prototype commercial scale “slow” dissolving batches. The release performance was dependent upon the extruder screw design, a key process parameter in scaling up the process from pilot to commercial scale. Four different lots of film-coated tablets (FCTs) were used in the modeling exercise: 150 mg (clinical batch_150 mg) and 450 mg (clinical batch_450 mg_fast) were manufactured at pilot scale, while a prototype final market image (FMI) 450 mg drug strength (clinical batch_450 mg_slow) was manufactured at commercial scale. The final drug product (FDP_450 mg) at a 450 mg dose was also granulated on a 50 mm extruder but with a different twin-screw design. Optimization of the pharmaceutical processing within the design space for the 450 mg final drug product (FDP) was performed selectively at a commercial scale.

The pilot scale 450 mg (clinical batch_450 mg_fast) was considered the reference batch as it was administered in Phase III clinical studies. Consequently, this batch was also used to build the biopharmaceutics model. Both the clinical batch_450 mg_fast and clinical batch_450 mg_slow were dosed in fasted healthy adults in a bioequivalence study; however, the FDP_450 mg was not tested/administered to patients.

Table I summarizes the clinical studies with the respective formulations which were utilized to build the biopharmaceutics model. The two formulations tested in the bioequivalence study (study B) were the 450 mg dose “fast” pilot scale and “slow” commercial scale (described above) immediate-release film-coated tablets.

Pharmacokinetic Data of Fevipiprant in Healthy Subjects

Two key clinical studies performed in fasted healthy adults were selected for biopharmaceutics modeling purposes (Table I). In the first study (study A), the absolute bioavailability was estimated to be approximately 40% based on a comparison of exposure from an oral dose of 150 mg fevipiprant (clinical_batch_150 mg) and an *i.v.* dose of 100 µg stable nonradioactive labeled fevipiprant ($^{13}\text{C}_2^{15}\text{N}_2$) administered one hour after the oral dosing to the same subjects ($n = 16$) by Weiss *et al.* (14). The study reports the bioavailability of QAW039 to be between 30 and 43%, depending on the calculation method. To further investigate this range, an advanced analysis of individual concentration time profiles by means of pharmacokinetic modeling and the AUC method was performed. Results of this analysis are provided in the Supplementary information (Part A) with a summary table (Supplementary Table S4) listing all modeling and calculation results. This assessment confirms that oral bioavailability of QAW039 is around 40%.

Analysis of the clinical data showed that P-glycoprotein did not have a relevant effect on oral absorption (14). The second trial (study B) was a confirmatory, open-label, randomized, two-sequence, two-period, crossover study in healthy subjects ($n = 108$, study on file) designed for exploring the bioequivalence between fevipiprant FCT batches at 450 mg produced at 2 different scales in healthy subjects ($n = 108$, study on file). While the geometric mean ratio (GMR) and confidence interval (CI) of AUC_{last} was 0.890 (0.860–0.920) for the two clinical batches (clinical_batch_450 mg_fast and clinical_batch_450 mg_slow), C_{max} GMR was 0.766 (0.717–0.819) and the two products did

not meet the bioequivalence criteria, specifically for C_{max} (CI within 0.80–1.25).

All clinical studies were performed in accordance with the ethical principles that have their origin in the declaration of Helsinki and were consistent with the International Conference on Harmonization/Good Clinical Practice (GCP) and applicable to regulatory requirements and the Novartis policy on Bioethics. In addition, dose-proportionality of fevipiprant was tested across various clinical studies in Caucasian and Japanese fasted healthy adults. All PK results (drug concentration in plasma *vs.* time) utilized for PBBM were within the dose-proportionality (data on file).

PBBM Approach

GastroPlus™ (version 9.8, Simulations Plus Inc., CA, USA) software with Advanced Compartmental Absorption Transit (ACAT™) model was utilized for simulating absorption, distribution, and elimination of the drug. Notably, the model simulated human microdose intravenous and oral data (BE and non-BE batches). The PBBM strategy is described in Fig. 1.

Table II summarizes the main physicochemical and pharmacokinetic parameters of fevipiprant focused on the model development.

Model Setup and Qualification

In the GastroPlus™ ACAT model describing the human GI tract, the default values for compartment volume percent occupation by water in the small intestine and colon (40% and 10%) were used for fasted state simulations. Human pharmacokinetic (PK) parameters were determined via a population pharmacokinetic (pop-PK) analysis of the pooled individual ($n = 16$) concentration time profiles from study A (14), as described in the Supplementary information (Part A). Input PK parameters to the biopharmaceutics model, such as plasma clearance and volume of distribution of

Table I Summary of Fevipiprant Clinical Study Arms Investigated in the Biopharmaceutics Model

Case study	Clinical study	Population (number of subjects)	Dose levels	Formulation	Unit dose
Study A	Absolute bioavailability study (14)	Caucasian ($n = 16$)	100 µg ¹	Liquid in vial	100 µg
			150 mg	Film-coated tablet – clinical_batch_150 mg	150 mg per tablet
Study B	BE study	Caucasian ($n = 108$)	450 mg	Film-coated tablet (pilot scale batch) – clinical_batch_450 mg_fast	450 mg per tablet
				Film-coated tablet (commercial scale batch) – clinical_batch_450 mg_slow	

¹Formulation administered intravenously

fevipiprant, were determined by fitting individual concentration time profiles after a single intravenous dose of 0.1 mg by a 2-compartment PK model with a linear clearance. Oral data were excluded from this fitting due to the clear impact of absorption parameters on distribution parameters (as described with model 1 and model 2 in the Supplementary information, Part A), therefore being less adequate as inputs to the biopharmaceutics model compared to the PK parameters derived from fitting intravenous data only. Table II lists PK and physicochemical input parameters to the GastroPlus™ model.

Drug absorption was simulated after the calculation of Peff and determination of physicochemical characteristics including drug solubility in biorelevant media (Table II) and aqueous buffers (Supplementary information, Part B). Integrated Peff was calculated by an in-house formula, which supported the use of CaCo-2 data.

Once disposition and physicochemical parameters were determined from *in vitro* and *in vivo* assessments, the model was utilized for simulating the observed data obtained from studies A and B with the clinical_batch_150 mg, clinical_batch_450 mg_fast, and clinical_batch_450 mg_slow, respectively. For all batches, the *in vivo* dissolution was investigated by utilizing *in vitro* dissolution, which was monitored using the quality control (QC) method. To demonstrate adequate discrimination between the non-BE batches investigated in study B, the sampling time point of 45 min was selected to describe the dissolution acceptance criteria. The *in vitro* testing conditions were determined at 900 mL (USP) phosphate buffer pH 6.8 (37°C) in a USP II apparatus with a rotation speed of 75 rpm. In all dissolution tests, the percent coefficient of variation (%CV) calculated at all-time points was not more than 5%. Therefore, the mean

dissolution profiles (i.e., % mean dissolved amount *vs.* time) with the three batches were initially fitted by following two approaches:

- Use of dissolution Takano model where dose, volume, and equilibrium solubility were considered for the *z*-factor calculations.
- Use of single Weibull function where the dosage form switched to CR: gastric release and the Weibull parameters of %total released, time scale factor, and shape were calculated. In this approach, there was no necessity for an immediate-release product to investigate either a gastric retention time in the ACAT physiology or a lag time in the Weibull function in order to fit the PK profiles. The formulations did not consist of excipients with gastro-resistant characteristics, and they were not incorporated into the biopharmaceutics model.

Adequacy of the fittings to the *in vitro* dissolution profiles was explored with *r* squared (R^2). Comparison of the two approaches led to the selection of the most predictive dissolution model, which was then utilized for reproducing the non-bioequivalence between the 450 mg clinical batches in study B. PK metrics in terms of C_{max} and AUC_{0-24h} calculations were provided by the GastroPlus™ software for all simulations. Prediction errors (%PE) were manually calculated based on the metrics.

Simulations performed for testing the virtual bioequivalence (VBE) of the slow *vs.* fast-dissolving batches at 450 mg incorporated a virtual population of 100 subjects which enrolled in a single virtual trial. In this population, the default coefficients of variation (%CV) were applied (i.e., the interindividual variability of the physiological parameters as

Fig. 1 PBBM strategy to define fevipiprant knowledge space and safe space

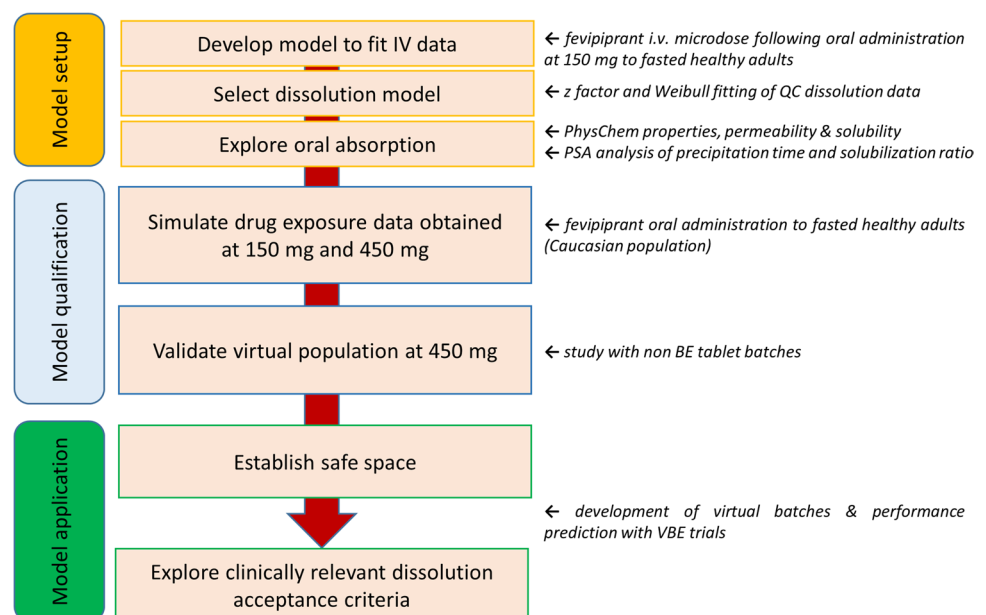


Table II Fevipiprant Physicochemical and Pharmacokinetic Parameters

Parameter	Value	Source/comment
Compound	Fevipiprant	
Mol wt	426.4 g/mol	Measured
Log P	2.36	Calculated with ADMET predictor
pKa	pKa ₁ : 2.9 (acidic), pKa ₂ : 4.1 (basic)	Determined after fitting pH-solubility profile. Estimated data were in line with experimental values
Sol_factors	193.2 for pKa ₁ and 772.9 for pKa ₂	Determined after fitting the pH-solubility profile
Biorelevant solubilities at 37°C	0.08 mg/ml in SGF (final pH 1.6 ¹) 1.1155 mg/ml in FaSSIF-V2 ² (final pH 6.3 ¹)	Determined when using the salt form
Solubilization ratio	17,600	Calculated in GastroPlus™ based on solubility in biorelevant media
Nanoparticle effect	Deactivated	No nanosized formulation investigated
Reference solubility	7.0E-3 mg/ml at pH 4	Determined when using the salt form
Precipitation time vs. pH	NA ³	Use of fixed (constant) value
Diffusion coefficient	0.66 × 10 ⁻⁵ cm ² /s	Calculated from the molecular weight in GastroPlus™
Drug particle density	1.2 g/ml	GastroPlus™ default value
Chemical degradation	Not taken into account	-
Human Peff	0.43 × 10 ⁻⁴ cm/s	Calculated by an in-house formula using Caco-2 data (internal data)
Blood/plasma conc. ratio	0.56	Internal data
Adj plasma Fup [%]	11.8	
CL [L/h]	18.7	Pop-PK analysis following an <i>i.v.</i> dose in combination with oral administration (14) – see Supplementary information, part A
Vc (L)	6.99	
Vp (L)	102	
Q [L/h]	8.37	
T _{1/2} [h]	12.31	
FPE [%]	37.1 ⁴	GastroPlus™ estimated value based on the derived CL value via population PK analysis

¹Reported pH indicates the values in the equilibrium

²The bile salts concentration was 3 mM for the FaSSIF-V2

³NA: not applicable

⁴Calculated using a body weight of 70 kg, CL of 33.4 L/h with blood to plasma ratio of 0.56, and the default GastroPlus™ liver blood flow rate

well as the PK parameters stored in the GastroPlus™ “population simulator” database for the healthy adult volunteers’ population).

Model Application to Define the Safe Space

Following development and qualification, the model was applied for the design of the safe space using the selected dissolution model (Fig. 1). Based on the outcome with the non-BE tablet batches, a batch with a slightly faster dissolution than the clinical batch_450 mg_slow (i.e., 73% dissolved at 45 min) could be bioequivalent to the clinical batch_450 mg_fast and reveal the lower boundary of the safe space. Likewise, another batch with a faster release than the clinical batch_450 mg_fast could reveal the upper boundary of the safe space.

For the lower boundary, virtual batches were calculated with the aim of meeting two potential acceptance criteria at 45 min sampling time point: (i) 80% dissolved

(virtual_batch_450_mg_80%) and (ii) 75% dissolved (virtual_batch_450_mg_75%). The faster dissolving virtual_batch_450_mg_80% needs a lower extent of dissolution to achieve marginal BE in C_{max} to the reference clinical batch_450 mg_fast, whereas the slower dissolving virtual_batch_450_mg_75% needs a higher extent of dissolution to fulfill the C_{max} BE criteria with the reference clinical batch_450 mg_fast (Fig. 7, inset pink curve vs. dashed red). Because the clinical batch_450 mg_slow met the BE criteria for AUC, dissolution extent with virtual_batch_450_mg_80% remained the same as with the slow dissolving clinical batch. For the virtual_batch_450_mg_75%, it is anticipated that although slower, dissolution might end with a higher %dissolved amount than that observed with the clinical batch_450 mg_slow to meet the BE criteria for C_{max}. For the upper boundary of the safe space, a virtual batch with an immediate complete release, i.e., behaving similarly to a solution form (Virtual batch_450 mg_100%), was utilized.

The design of the virtual batches was based on PSAs performed with the dissolution-related parameters for the clinical batch_450 mg_slow. The clinical relevance of the proposed acceptance criteria was evaluated with VBE crossover trials between the virtual_batch_450 mg_80%, virtual_batch_450 mg_75%, and the clinical batch_450 mg_fast. Population results with those batches revealed the lower boundary of the safe space. For the upper boundary, the BE trial between the virtual_batch_100% and the FDP_450 mg, which exhibited slower dissolution than the clinical batch_450 mg_fast, was investigated. For all simulations, a virtual population of 100 subjects was selected and the default %CV was applied. The population simulations were performed as single trials.

Results

GastroPlus™ Model Setup and Qualification

Dissolution data fitted with the z -factor or Weibull function at 150 mg and 450 mg dose levels are shown in Fig. 2. Dissolution rate and extent with clinical batch_150 mg were adequately captured using both dissolution models. Similarly, at 450 mg dose level, fitting with both models was adequate for the clinical batch_450 mg_fast. Conversely, the dissolution extent for the clinical batch_450 mg_slow was overestimated when utilizing the Takano model. Further to the dissolution model suitability, although AUC CI range in study B was within the BE criteria, the point estimate was 0.89 and the estimated upper limit was 0.92. Interestingly, those statistical analysis results were in line with the estimated 88% and 100% drug amount dissolved via Weibull simulations for the slow-dissolving batch and the fast-dissolving batch (Fig. 2). Distinct from the Johnson model, the Takano model would incorporate the solubilities in aqueous media and z factors into the calculations for the dissolution rate. Consequently, Takano model simulations

would result in complete *in vivo* dissolution for all batches, including the slow-dissolving clinical batch. Therefore, the Weibull function (CR release dosage form) was utilized for further investigations, where fittings reflected all dissolution curves as well as the anticipated *in vivo* dissolution profiles described hereafter.

Upon selection of the dissolution model, 3D parameter sensitivity analyses (PSAs) were performed with the clinical batch_150 mg and clinical batch_450 mg_fast to investigate the impact of the Weibull time scale factor and permeability on C_{max} (Fig. 3). For both dose levels, while C_{max} is highly sensitive to drug permeability, a slight drop down is also observed when dissolution with fevipiprant drug products becomes slower. This finding that the slow-dissolving batch also had a slower absorption rate could explain the outcome of the unsuccessful bioequivalence between the clinical batch_450 mg_fast and the clinical batch_450 mg_slow. In such a case, formulation efforts were focused on the process (i.e., twin-screw melt granulation) and scale-up parameters to ensure dissolution performance of the formulation (including the FDP) is within the safe space coverage.

Further to model setup and qualification, based on the solubility calculated in each physiological region, it can be assumed that drug solubility is mainly driven by the pH (Supplementary information, Part C). Consequently, drug precipitation is likely to occur upon the drug transfer to the caecum, particularly for the higher dose level of 450 mg. On the other hand, clinical data previously collected for measuring the caecal pH in fasted healthy adults following colonoscopy showed that the median value is 7.4 (range: 6.2–8.5) (15). Conversely, ACAT physiology considers a pH value of 6.4 for the caecal compartment. According to the clinical observation, fevipiprant solubility should be increasing to 2.965 mg/ml instead of 0.7190 mg/ml as calculated for the caecum by the ACAT model. In this case, no precipitation with a fevipiprant is expected. Similarly, Litou *et al.* showed that the median duodenal pH of samples aspirated 5 min, 15 min, 30 min, and 50 min post-water administration

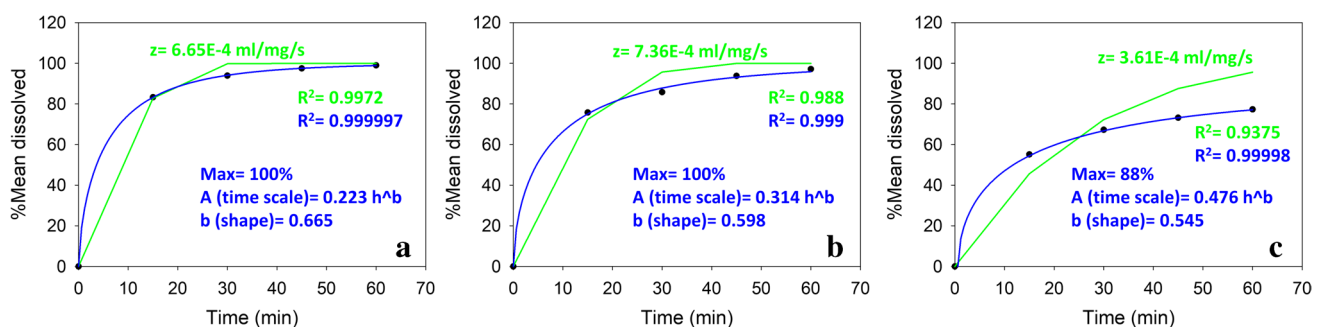


Fig. 2 z -factor (solid green lines) and Weibull fittings (solid blue continuous lines) of experimental %Mean ($n=6$) dissolved amount vs. time (filled circles) for clinical batch_150 mg (a), clinical batch_450

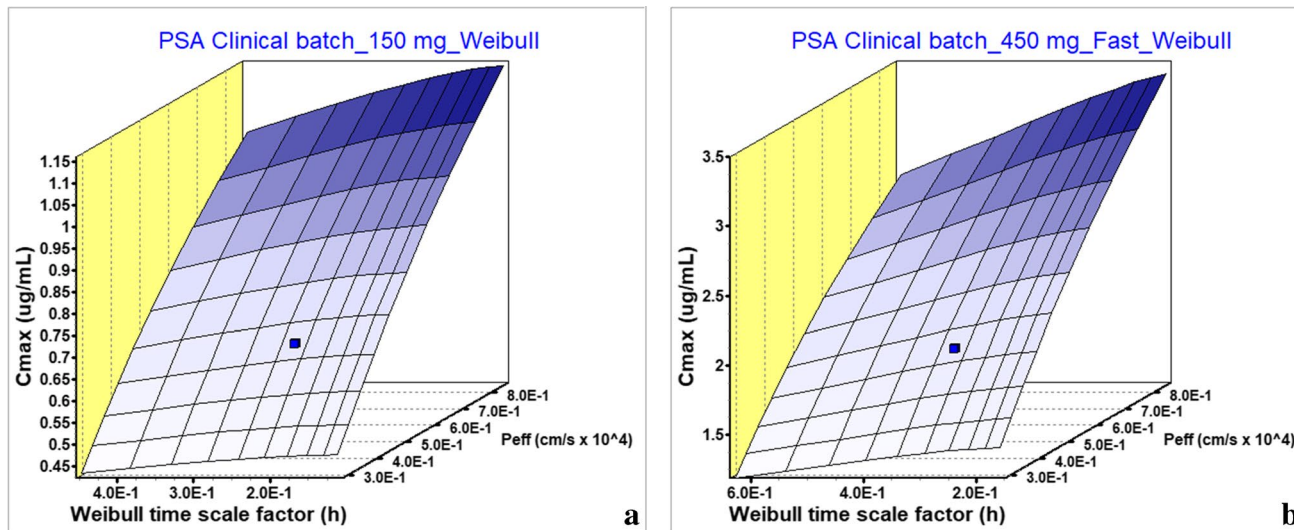
mg_fast (b), and clinical batch_450 mg_slow, non-BE (c). Insets: calculated z -factor and Weibull parameters

were 6.8, 6.2, 6.3, and 6.5, respectively (16). In this context, duodenal drug solubility should be increased to 1.71 mg/ml instead of 0.545 mg/ml if the pH in the duodenal compartment is 6.5. Therefore, for the model to constitute those physiological parameter changes, the precipitation time was optimized to 90,000 s in all simulations. Interestingly, simulation results were similar to the outcome obtained when the pH in the duodenum and jejunum was changed to 6.5 and in the caecum to 7.4 for model training purposes (Supplementary information, Part D).

Single simulations with the clinical batches tested in studies A and B showed complete release and limited absorption (Fig. 4). As a result, the absolute bioavailability (*F*) was estimated at 45% approximately that is in line with other investigated methods (Supplementary Table S4; Supplementary information, Part A). In addition, exposure profiles were aligned with the clinical observations (Fig. 4). For the clinical batch_150 mg, the prediction errors for C_{max} and AUC_t were 6.6% (obs.: 724 ng/ml vs. pred.: 676 ng/ml) and 1.23% (obs.: 3210 ng × h/ml vs. pred.: 3250 ng × h/ml), respectively. For the clinical batch_450 mg_fast, the prediction errors for C_{max} and AUC_t were 1.41% (obs.: 1980 ng/ml vs. 1952 ng/ml) and 5.8% (obs.: 9200 ng × h/ml vs. pred.: 9730 ng × h/ml), respectively. For the clinical batch_450 mg_slow, the prediction errors for C_{max} and AUC_t were 2.9% (obs.: 1550 ng/ml vs. pred.: 1595 ng/ml) and 4.4% (obs.: 8216 ng × h/ml vs. 8568 ng × h/ml), respectively. In all cases, simulated T_{max} was within the observed range of the

median values (i.e., from 1.5 to 2 h). It must be noted that despite the low drug solubility estimated in the acidic conditions, the model detected higher dissolved drug amounts in the stomach than solubility would allow. However, for all three dosage forms, preliminary simulations indicated a minimal impact of the gastric drug concentrations on the drug absorption and exposure, respectively (Supplementary information, Part E).

VBE results with the slow and fast-dissolving clinical batches at 450 mg are shown in Fig. 5. To ensure limited dissolution for the clinical batch_450 mg_slow, the %CV for the Weibull “Max. (total released) (%)” parameter was nullified. Likewise, due to the low drug solubility in the caecum, the precipitation time was not considered in the simulations. Preliminary simulations confirmed that the virtual population utilized for the VBE trial was equivalent to the experimental PK data (Supplementary information, Part F). Moreover, the analysis of in-transformed VBE data showed that the two formulations are non-bioequivalent. As observed in study B, the C_{max} did not meet the BE criteria. While GMR was close to the lower BE limit (0.814), 90% CI was out of the range of acceptance criteria (0.756–0.876). On the other hand, GMR AUC_t was 0.879 and 90% CI was 0.838–0.922. In addition, virtual simulations matched the observed CI; i.e., for both C_{max} and AUC , the difference calculated between the upper and lower limit was close to the respective clinical difference. Further to qualification, the model adequately reflected the plasma PK of fevipiprant



1

Fig. 3 PSA surface plots of fevipiprant with clinical batch_150 mg_Weibull (a) and clinical_450 mg_fast_Weibull (b). The blue-filled square represents the baseline

following single-dose administrations with capsules or FCTs to fasted healthy adults in the dose range of 10–500 mg (Supplementary information, Part G).

Model Application to Define the PBBM Safe Space

An indicative dissolution time scale factor ($A; h^{-b}$) sensitivity analysis with the clinical batch_450 mg_slow is shown in Fig. 6. According to this analysis, the Weibull time scale factor was calculated at 0.35 (virtual_batch_450 mg_80%) for a virtual batch that exhibited 80% amount dissolved at 45 min and 88% maximum amount dissolved across the gastrointestinal tract (i.e., Weibull max amount dissolved; Fig. 6a). Interestingly, the C_{max} ratio between the virtual_batch_450 mg_80% and clinical batch_450 mg_fast was calculated at 0.868 (i.e., equivalent to a 13% difference in the mean C_{max} ; Supplementary information, Part H). Therefore, considering the longest C_{max} ratio distance in the virtual population trial (Fig. 5), where 7 points approx. were calculated from the point estimate to the higher limit of the 90% CI, it is then anticipated that the

batches will be bioequivalent when tested in a virtual crossover single trial. In this case, the lower limit of the 90% CI for the C_{max} ratio should be close to 0.8. In addition to the BE calculations, it can also be implied that AUC ratios will be meeting the acceptance criteria which were previously fulfilled for the clinical batch_450 mg_slow, where the maximum amount dissolved was the same as with that of the virtual_batch_450 mg_80% (i.e., 88% at 60 min; Fig. 2c).

Further to the results, an indicative PSA to C_{max} performed with the scale factor when the Weibull max ranged from 85 to 100% revealed the virtual_batch_450 mg_75% which exhibited 75% amount dissolved at 45 min. The maximum amount dissolved was calculated at 100% while the time scale factor was 0.61 (Fig. 6b1). Dissolution parameters with this batch matched the C_{max} which was estimated for the virtual_batch_450 mg_80%. Because the PSA indicated complete dissolution, the sensitivity of the Weibull max and the scale factor to AUC_t was also investigated (Fig. 6b2). As anticipated, exposure was higher when increasing the dissolution extent from 85 to 100% amount dissolved.

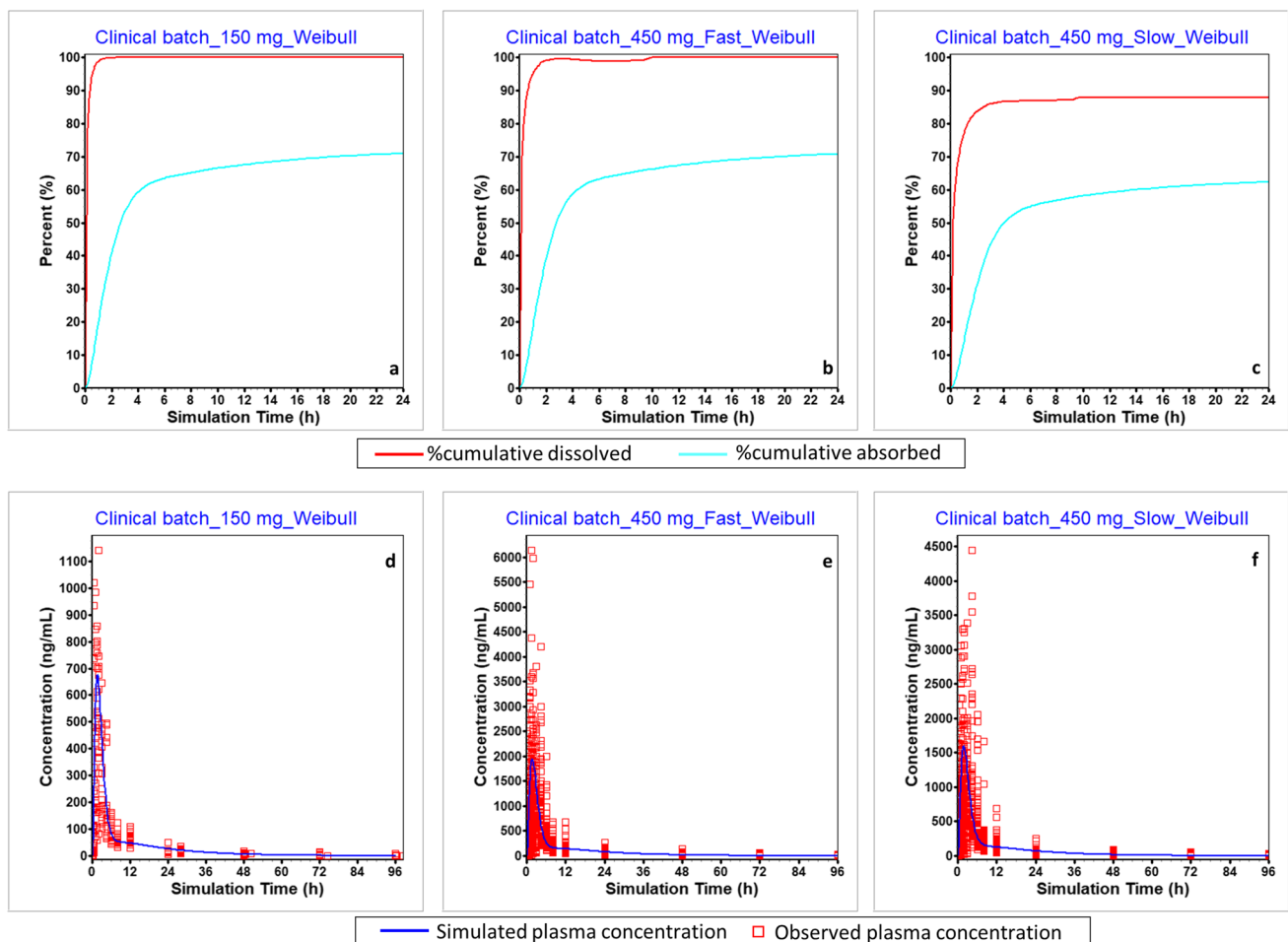
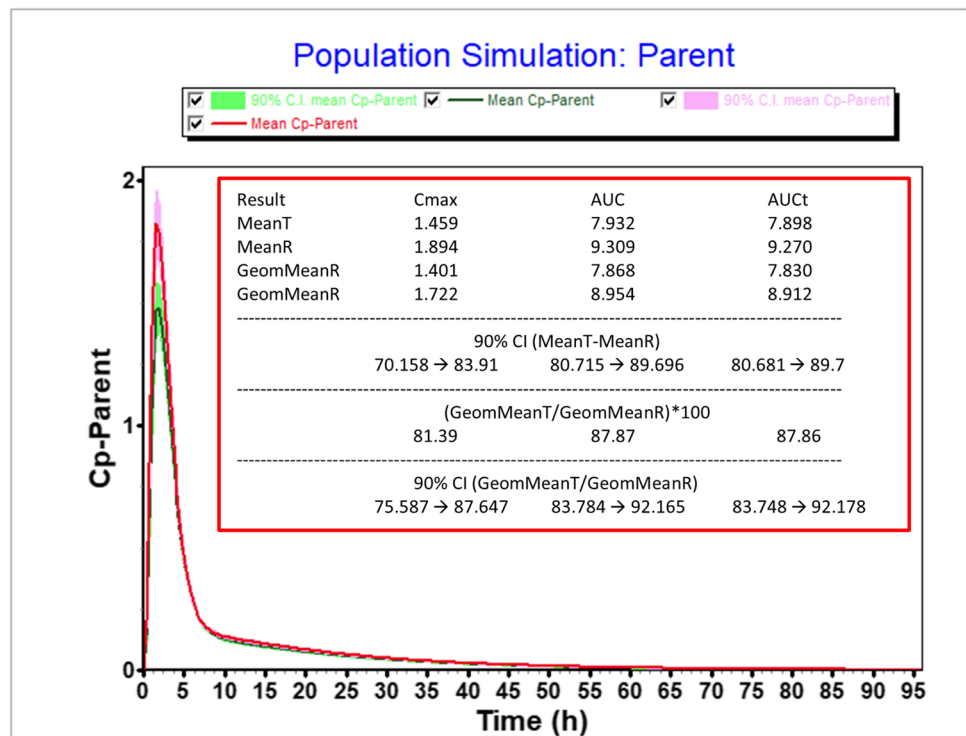


Fig. 4 Simulated %cumulative dissolved (red line) or absorbed (light blue line) amounts vs. time profiles (a, b, c) and the simulated C_p vs. time profiles (blue lines; d, e, f) for clinical batch_150 mg

(study A; a, d), clinical batch_450 mg_fast (study B; b, e), and clinical batch_450 mg_slow, non-BE (study B; c, f). Open squares are the observed individual C_p time profiles

Fig. 5 Virtual population simulation plot ($n=100$ subjects) with plotted results of two population simulations and the comparison of these two trials (inset: In-transformed PK parameters). Population simulations indicated with green color were performed with the test clinical batch_450 mg_slow. Population simulations indicated with red color were performed with the reference clinical batch_450 mg_fast



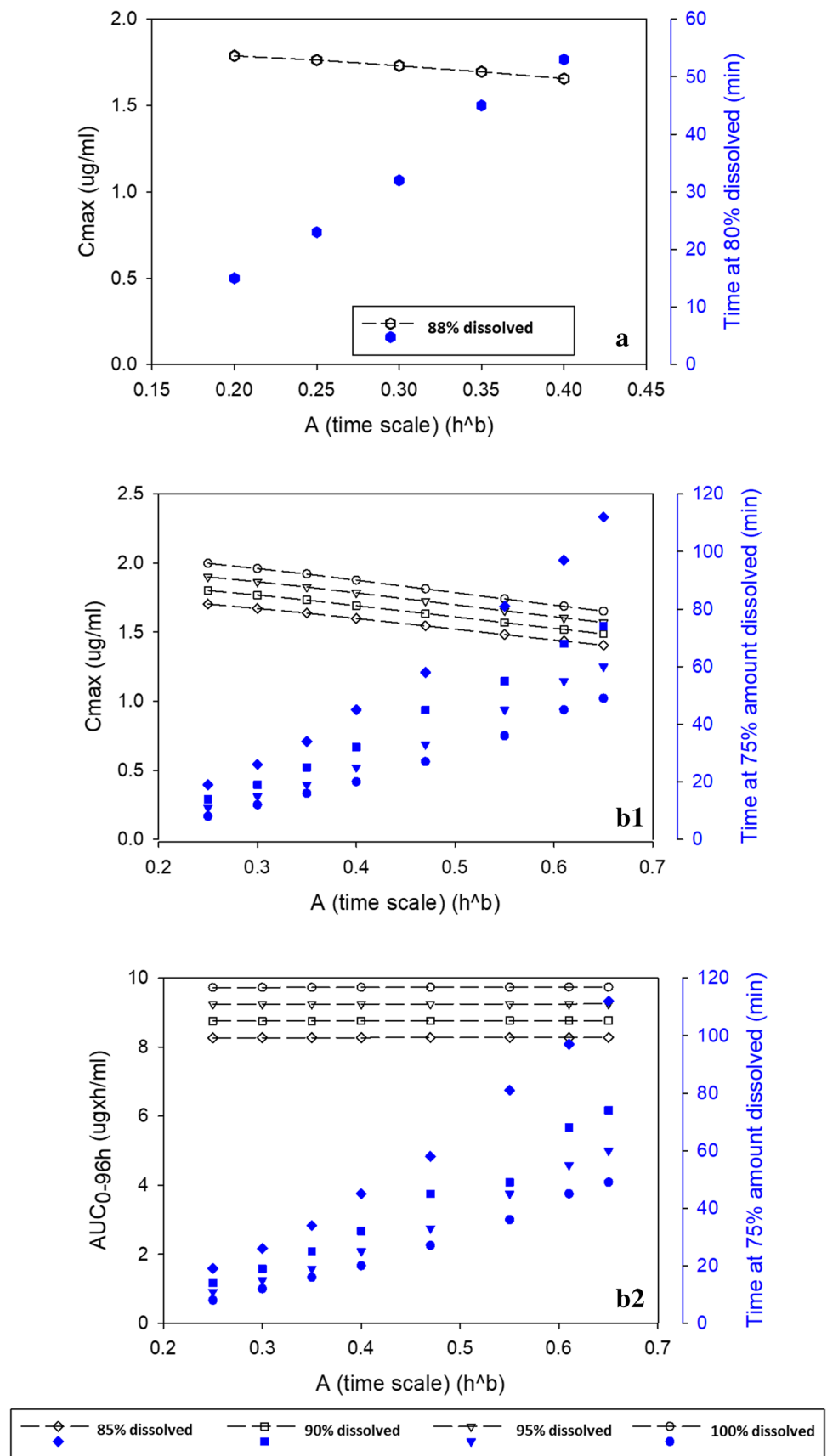
A third virtual batch with the fastest possible release (i.e., $A=0.01 h^b$) and 100% max amount dissolved was utilized (virtual_batch_450 mg_100%) to explore the upper end of the safe space. For all virtual batches, the Weibull shape parameter remained the same as with that calculated for the clinical_batch_450 mg_slow (i.e., 0.545). Further to the calculated dissolution profiles, an adequate fitting of the QC dissolution data with FDP_450 mg using the single Weibull equation was obtained (diamonds in Fig. 7). The maximum dissolved amount was estimated at 96%, while the time scale factor and the shape were 0.333 h^b and 0.598, respectively.

The lower boundary of the safe space is defined by the dissolution profiles of the virtual_batch_450 mg_80% and the virtual_batch_450 mg_75%, whichever is lower, represented by the green area in Fig. 7. Hereby, the virtual_batch_450 mg_80% represents a batch with an adequately fast, but incomplete dissolution. virtual_batch_450 mg_75% represents a batch with slow but complete dissolution. Any dissolution profile which passes a white space below this safe space, even if only for a fraction of time, is bioinequivalent. This is demonstrated by the clinical_batch_450 mg_slow, which is covered by the safe space within the first 30 min but leaves it in the time period of 30 min to approximately 6 h and re-enters the safe space afterward. The virtual bioequivalence trials between virtual_batch_450 mg_80%, clinical_batch_450 mg_fast and virtual_batch_450 mg_75%, clinical_batch_450 mg_fast confirmed the lower boundary of the safe space (Fig. 7). As with previous VBE trials, to reflect the dissolution extent calculated for all batches, the

“Max. (total released) (%)” parameter was nullified. Likewise, the precipitation time was not taken into account in the population simulations. For both geometrical mean C_{max} and AUC ratios, the lower limits in the 90% CI were equal to or close to 0.8 (Table III).

In addition, the virtual bioequivalence trial between the virtual_batch_450 mg_100% and the FDP_450 mg confirmed the upper end of the safe space (Fig. 7 and Table III). Further to this simulation, clinical evidence showed that absorption of 450 mg fevipiprant was not impacted by co-administration of an acid-reducing agent in fasted healthy adults. As a result, a slight increase in fevipiprant peak exposures was observed in the presence of famotidine (12%), although no concurrent change in total fevipiprant exposure was observed (clinical data on file). Therefore, it can be concluded that absorption is not impacted when gastric pH increases and the dissolution rate for fevipiprant becomes faster. Furthermore, it shall be noted that administration of famotidine in the fasted state may result in a maximal effect of increasing basal gastric pH. Litou *et al.* showed that during 35 min post-water administration under achlorhydric conditions, median (range) pH values are 7.1 (5.0–7.3) (16). In the presence of an acid-reducing agent (ARA) such as famotidine, fevipiprant solubility increases in this pH range and the dissolution rate in the stomach is expected to be similar to that in the small intestine. Because the FDP batch at 450 mg exhibited faster dissolution than that calculated with the slow-dissolving virtual batches, the dissolution profile was within the safe space (Fig. 7). The ARA study

Fig. 6 C_{max} (ug/ml) (**a, b1**) and AUC_{0-96h} (ug×h/ml) (○) with time at 80% dissolved (min) or Weibull max vs. A (time scale factor) when Weibull max was 88% (**a**) or changed (**b1, b2**) to 85% (diamonds), 90% (squares), 95% (triangles), and 100% (circles). The shape b was set at 0.545. Unfilled circles correspond to the left y-axis, while filled circles correspond to the right y-axis



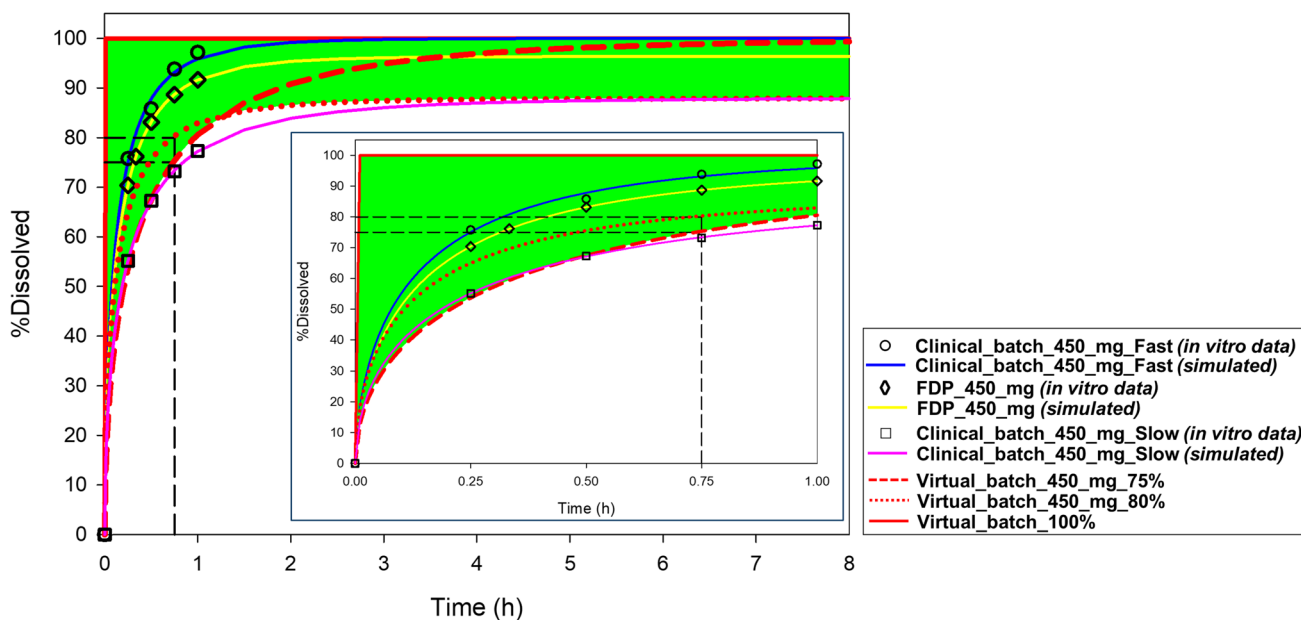


Fig. 7 Bioequivalence safe space plot including the clinically tested dissolution knowledge space; calculated dissolution profiles for virtual_batch_100% (continuous red line), virtual_batch_450_mg_80% (dotted red line), virtual_batch_450_mg_75% (medium dashed red line), and FDP_450 mg using the single Weibull equation (solid pink line). For comparative purposes, % mean experimental ($n=6$; symbols) and fitted dissolved amount (solid lines) vs. time with clinical

batch_450 mg_fast (circles; solid blue line), clinical batch_450 mg_slow (squares; solid pink line), and FDP_450 mg (diamonds) are also presented. The blue and pink solid lines define the IR knowledge space. The green area represents the safe space for fevipiprant at the dose level of 450 mg. Inset: fittings of experimental % dissolved amounts calculated up to 1 h

results provided circumstantial evidence that a faster dissolution can reside within the safe space. Furthermore, bioequivalence between FDP_450 mg and virtual_batch_450 mg_100% was also confirmed via a virtual population single trial (Table III). Geometrical mean ratios for both C_{max} and AUC were higher than the ratios calculated between the virtual_batch_450 mg_80% and the clinical batch_450 mg_fast.

Discussion

The calculation of two lower boundary profiles led to the establishment of two differing safe spaces possessing different lower boundaries. A combination of both analyses, as

demonstrated in Fig. 7, shows that the most representative dissolution specification would be the intersection point at the lower boundary profiles. This point is located at 1.3 h and is considered not applicable for an immediate-release formulation. In this case, the safe space analysis could reveal an alternative specification located at 60 min time point and calculate the lowest possible amount dissolved that is matching the profile of the virtual_batch_75%. For this batch, 81% amount dissolved was calculated. Therefore, a specification of $Q=80\%$ amount dissolved in 60 min or less adequately defines the boundary of the safe space for an IR oral solid dosage form.

Although fevipiprant safe space showed that both proposed dissolution acceptance criteria are clinically relevant,

Table III Virtual BE Results ($n=100$ Subjects) Between Test Batches Virtual_Batch_450 mg_100%, Virtual_Batch_450 mg_80%, Virtual_Batch_450 mg_75%, FDP_450 mg, and Reference Batch Clinical Batch_450 mg_Fast

Reference batch	Test batch	Predicted C_{max}		Predicted AUC_{0-t}	
		Geomean ratio	90% CI	Geomean ratio	90% CI
Clinical batch_450 mg_fast ¹	Virtual_batch_450 mg_80%	0.865	0.806–0.929	0.883	0.846–0.921
Clinical batch_450 mg_fast ¹	Virtual_batch_450 mg_75%	0.863	0.801–0.929	1.00	0.933–1.074
FDP_450 mg ²	Virtual_batch_450 mg_100%	1.065	0.984–1.152	0.996	0.933–1.062

¹Pilot scale batch

²Commercial batch

the dissolution similarity (f_2) factors calculated with the commercial scale batch *vs.* the fastest or slowest dissolving virtual batches did not meet the requirements (Supplementary information, Part I). Traditionally, the 10% range may provide some guidance to formulators during the formulation and/or process optimization. However, for fevipiprant, the differences in the dissolved amounts between the reference and those test batches exceeded 10%. Furthermore, the f_2 methodology was not applicable for evaluating the very rapid dissolving virtual_batch_100% *vs.* the rapid dissolving commercial scale batch as there were less than two data points equal to or below 85% of the drug dissolved for the virtual_batch_100%. For fevipiprant, the safe space indicated *in vivo* relevance for the dissolution differences between those two batches. Especially for BCS Class IV drug candidates, it can be concluded that absorption may be driven mainly by the permeability or solubility rather than the dissolution rate. In this case, PBBM may supersede f_2 methodology, and the construction of a safe space may allow a larger than 10% dissolution difference for bioequivalent batches.

The existing business case for fevipiprant shows that drug absorption for rapidly dissolving formulations at 450 mg is controlled by permeation, while absorption for formulations with slower dissolution is also impacted by the dissolution rate. Interestingly, the current business case can be further applied for other compounds with comparable physicochemical and biopharmaceutical characteristics, especially for waiving a BE study based on simulation and modeling, but at least for process and site changes, when the dissolution similarity approach failed. However, it is vital for applicants and sponsors to design those experiments which would allow them to develop a robust and reliable biopharmaceutics model. For instance, PK analysis of *i.v.* data in combination with oral PK would allow accurate characterizing of the clearance and the distribution parameters and, in parallel, to verify the drug PK linearity. According to the draft guidance issued for physiologically based pharmacokinetic analyses by FDA (7), to increase the confidence of the biopharmaceutics model, it is strongly recommended to demonstrate the model's predictive performance based on PK data from batches exhibiting an unacceptable bioavailability (BA), in addition to those exhibiting acceptable BA (compared to a target and/or reference product). In this context, BA would be considered unacceptable when, based on BE criteria, the 90 percent confidence interval of the test-to-reference geometric mean ratio of C_{\max} and AUC falls outside the range of 80 to 125 percent.

In addition to the drug disposition parameters, special attention shall be paid to the drug absorption phase. Depending on the drug's physicochemical properties as well as the drug product characteristics, a biorelevant dissolution method should be identified and supported by the

observed PK data. That method is a key modeling input because it probes both the extent and rate of *in vivo* drug product release. An extensive list of biorelevant media and testing conditions have been previously described in the literature (17). Nevertheless, the selection of the biorelevant method as well as the development of the QC method should be specifically linked to the quality of the drug product characteristics. For fevipiprant, an *in vitro* two-stage biorelevant dissolution protocol was utilized for the clinical_batch_450 mg_fast and clinical_batch_450 mg_slow, respectively (Supplementary information, Part J). In the second stage, dissolution differences were in line with the QC data. This observation is the link between a biorelevant dissolution method based on the two-stage method and the QC method. Also, biorelevant two-stage dissolution data matched the observed exposure when the profiles were successfully fitted with the triple Weibull equation.

After collecting the *in vitro* dissolution data, various integration methods to the biopharmaceutics model can be utilized. *In silico* platforms can apply the Johnson, Takano, and Weibull functions (18–20). Although the key input parameter is the particle size distribution (PSD) for the Johnson dissolution model, Pepin *et al.* showed an alternative approach to fit the dissolution profile by reproducing a PSD dataset (8). This virtual dataset is then integrated within the model for predicting the *in vivo* dissolution rate. However, for this exercise, additional information such as the interfacial tension or the apparent drug solubility with surfactant (in the case of solubilizers) is often needed. The Takano dissolution model allows for the direct integration of multiple or single dissolution profiles when the dose, the volume, and the drug solubility in the investigated media are known. In this circumstance, it should be noted that fitting of the dissolution profile can be inadequate if dissolution for a drug product is incomplete, while the solubility input parameter allows for achieving the sink conditions. Thus, the Takano dissolution model might result in an unacceptable dissolution profile fitting that might be misleading. Finally, although the Weibull function is extensively used for modified release formulations, few cases have shown the usefulness of the dissolution model for IR formulations allowing for more flexibility in the case of incomplete dissolution (10, 11, 21). In principle, the function offers the possibility to fit dissolution data exhibiting single or multiple phases and to directly link the *in vivo* performance and safe space with the quality control method. A lag time may be considered for the fitting when the Weibull function is used. It is acknowledged that often an *in vitro* dissolution profile in non-biorelevant media as used for QC purposes does not correctly reflect the environmental situation in the GI tract, but in certain cases, the release

characteristics in such a dissolution medium adequately reflect the *in vivo* dissolution behavior, especially when supported by PBBM. This is mainly true for compounds that exhibit a dissolution/solubility-controlled absorption when dissolution conditions were selected with a comparable release mechanism *in vitro* and *in vivo*, as it is the prerequisite for IVIVC approaches.

Conclusions

A physiology-based biopharmaceutics model (PBBM) was built for fevipiprant after the collection of plasma concentration time data describing *i.v.* (100 mg) and oral (150 mg and 450 mg) administrations in fasted healthy subjects. The model was validated by using PK data obtained from batches exhibiting an unacceptable BE. For this exercise, the Takano and Weibull functions were applied for integrating the QC dissolution data into the model. Model fitting using the Takano function was not adequate for the formulation at 450 mg, which exhibited a limited extent of dissolution. Therefore, modeling was progressed using the Weibull function, which successfully described the dissolution profiles observed with all formulations.

Following model qualification, a safe space was applied by using time-scaled-down virtual batches, which exhibited 80% or 75% dissolution at 45 min. Virtual population simulations showed that both batches ensured bioequivalence to the pivotal clinical batch (clinical batch_450 mg_fast) or the commercial scale batch (FDP_450 mg). A combination of safe space analyses resulted in a specification of Q = 80% amount dissolved in 60 min or less for fevipiprant IR oral solid dosage form. Furthermore, dissolution with the commercial batch at 450 mg was well within the anticipated bioequivalence space, confirming that the PK performance of the commercial scale batch is similar to that investigated in clinics.

A 3D PSA showed that fevipiprant absorption is mainly impacted by intestinal permeability at 150 mg. At 450 mg, absorption is also impacted by the dissolution rate, which could explain the outcome of the unacceptable BE. In fact, the slow-dissolving clinical batch exhibited incomplete dissolution when the formulation was tested with the QC method. Overall, this case study illustrates that, especially for BCS IV drugs, PBBM may offer new opportunities to demonstrate similar *in vivo* performances arising from process parameters, including scaling up, filling the gap for drug products that are not covered by BCS-based or IVIVC-based biowaivers, but are a subject of a dissolution safe space approach.

Supplementary Information The online version contains supplementary material available at <https://doi.org/10.1208/s12248-023-00787-5>.

Acknowledgements The authors acknowledge numerous Novartis colleagues who contributed to the development of fevipiprant/QAW039. Fevipiprant was discovered by Novartis Institutes for BioMedical Research.

Author Contribution All authors contributed to the conception and design of the work, drafting/revising of the content, and final approval of the version to be published.

AK, MG, WL, SSD, CS-L, TH: generation of experimental data and its curation, writing/revising content, and final editing of the version to be published.

Data Availability The datasets generated or analyzed during this study, beyond what has been shared in this publication, are not publicly available as they are proprietary to Novartis AG. Reasonable requests to the corresponding author may be supported.

Declarations

Conflict of Interest The authors declare no competing interests.

References

- Kostewicz ES, Abrahamsson B, Brewster M, Brouwers J, Butler J, Carlet S, *et al.* In vitro models for the prediction of in vivo performance of oral dosage forms. *Eur J Pharm Sci.* 2014;57:342–66. <https://doi.org/10.1016/j.ejps.2013.08.024>.
- Kostewicz ES, Aarons L, Bergstrand M, Bolger MB, Galetin A, Hatley O, *et al.* PBPK models for the prediction of in vivo performance of oral dosage forms. *Eur J Pharm Sci.* 2014;57:300–21. <https://doi.org/10.1016/j.ejps.2013.09.008>.
- Margolske A, Darwich AS, Pepin X, Aarons L, Galetin A, Rostami-Hodjegan A, *et al.* IMI - Oral biopharmaceutics tools project – evaluation of bottom-up PBPK prediction success part 2: an introduction to the simulation exercise and overview of results. *Eur J Pharm Sci.* 2017;96:610–25. <https://doi.org/10.1016/j.ejps.2016.10.036>.
- Mitra A, Suarez-Sharp S, Pepin XJH, Flanagan T, Zhao Y, Kotzagiorgis E, *et al.* Applications of physiologically based biopharmaceutics modeling (PBBM) to support drug product quality: a workshop summary report. *J Pharm Sci.* 2021;110(2):594–609. <https://doi.org/10.1016/j.xphs.2020.10.059>.
- Abend A, Heimbach T, Cohen M, Kesisoglou F, Pepin X, Suarez-Sharp S. Dissolution and translational modeling strategies enabling patient-centric drug product development: the M-CERSI workshop summary report. *AAPS J.* 2018;20(3):60. <https://doi.org/10.1208/s12248-018-0213-x>.
- Suarez-Sharp S, Cohen M, Kesisoglou F, Abend A, Marroum P, Delvadia P, *et al.* Applications of clinically relevant dissolution testing: workshop summary report. *AAPS J.* 2018;20(6):93. <https://doi.org/10.1208/s12248-018-0252-3>.
- The use of physiologically based pharmacokinetic analyses – biopharmaceutics applications for oral drug product development, manufacturing changes, and controls. FDA draft guidance. FDA-2020-D-1517-0002. 2020. <https://www.regulations.gov/document/FDA-2020-D-1517-0002>. Accessed Sept 2022.
- Pepin XJ, Flanagan TR, Holt DJ, Eidelman A, Treacy D, Rowlings CE. Justification of drug product dissolution rate and drug substance particle size specifications based on absorption PBPK modeling for lesinurad immediate release tablets. *Mol Pharm.* 2016;13(9):3256–69. <https://doi.org/10.1021/acs.molpharmaceut.6b00497>.
- Loisios-Konstantinidis I, Cristofolletti R, Fotaki N, Turner DB, Dressman J. Establishing virtual bioequivalence and clinically relevant specifications using *in vitro* biorelevant dissolution testing

- and physiologically-based population pharmacokinetic modeling. Case example: Naproxen. *Eur J Pharm Sci.* 2020;143:105170. <https://doi.org/10.1016/j.ejps.2019.105170>.
10. Heimbach T, Kesisoglou F, Novakovic J, Tistaert C, Mueller-Zsigmondy M, Kollipara S, *et al.* Establishing the bioequivalence safe space for immediate-release oral dosage forms using physiologically based biopharmaceutics modeling (PBBM): case studies *J Pharm Sci.* 2021;110. <https://doi.org/10.1016/j.xphs.2021.09.017>.
 11. Laisney M, Heimbach T, Mueller-Zsigmondy M, Blumenstein L, Costa R, Ji Y. Physiologically based biopharmaceutics modeling to demonstrate virtual bioequivalence and bioequivalence safe-space for ribociclib which has permeation rate-controlled absorption. *J Pharm Sci.* 2021;111(1):274–84. <https://doi.org/10.1016/j.xphs.2021.10.017>.
 12. Pearson D, Weiss HM, Jin Y, Jaap van Lier J, Erpenbeck VJ, Glaenzel U, *et al.* Absorption, distribution, metabolism, and excretion of the oral prostaglandin D2 receptor 2 antagonist fevipiprant (QAW039) in healthy volunteers and *in vitro*. *Drug Metab Dispos.* 2017;45(7):817–25. <https://doi.org/10.1124/dmd.117.075358>.
 13. Martin CV, Stocker S, Bautista M, Rogue V, Steib-Lauer C, Häcker H-G, *et al.* Commercial scale transfer of a twin-screw melt granulation process for high drug load fevipiprant tablets. *Drug Dev Ind Pharm.* 2022;48(5):211–25. <https://doi.org/10.1080/03639045.2022.2104307>.
 14. Weiss HM, Umehara K, Erpenbeck VJ, Cain M, Vemula J, Elbast W, *et al.* A study of the effect of cyclosporine on fevipiprant pharmacokinetics and its absolute bioavailability using an intravenous microdose approach. *Drug Metab Dispos.* 2020;48(10):917–24. <https://doi.org/10.1124/dmd.120.090852>.
 15. Reppas C, Karatza E, Goumas C, Markopoulos C, Vertzoni M. Characterization of contents of distal ileum and cecum to which drugs/drug products are exposed during bioavailability/bioequivalence studies in healthy adults. *Pharm Res.* 2015;32:3338–49. <https://doi.org/10.1007/s11095-015-1710-6>.
 16. Litou C, Vertzoni M, Goumas C, Vasdekis V, Xu W, Kesisoglou F, *et al.* Characteristics of the human upper gastrointestinal contents in the fasted state under hypo- and achlorhydric gastric conditions under conditions of typical drug-drug interaction studies. *Pharm Res.* 2016;33:1399–412. <https://doi.org/10.1007/s11095-016-1882-8>.
 17. Andreas CJ, Rosenberger J, Butler J, Augustijns P, McAllister M, Abrahamsson B, *et al.* Introduction to the OrBiTo decision tree to select the most appropriate *in vitro* methodology for release testing of solid oral dosage forms during development. *Eur J Pharm Biopharm.* 2018;130:207–13. <https://doi.org/10.1016/j.ejpb.2018.07.003>.
 18. Lu AT, Frisella ME, Johnson KC. Dissolution modeling: factors affecting the dissolution rates of polydisperse powders. *Pharm Res.* 1993;10:1308–14. <https://doi.org/10.1023/a:1018917729477>.
 19. Takano R, Sugano K, Higashida A, Hayashi Y, Machida M, Aso Y, *et al.* Oral absorption of poorly water-soluble drugs: computer simulation of fraction absorbed in humans from a miniscale dissolution test. *Pharm Res.* 2006;23:1144–56. <https://doi.org/10.1007/s11095-006-0162-4>.
 20. Langenbucher F. Letters to the Editor: Linearization of dissolution rate curves by the Weibull distribution. *J Pharm Pharmacol.* 1972;24:979–81. <https://doi.org/10.1111/j.2042-7158.1972.tb08930.x>.
 21. Bhattiprolu AK, Kollipara S, T A, Boddu R, S C. Utility of physiologically based biopharmaceutics modeling (PBBM) in regulatory perspective: application to supersede f2, enabling biowaivers & creation of dissolution safe space. *J Pharm Sci.* 2022;S0022–3549(22):00399–9. <https://doi.org/10.1016/j.xphs.2022.09.003>.

Publisher's Note Springer Nature remains neutral with regard to jurisdictional claims in published maps and institutional affiliations.

Springer Nature or its licensor (e.g. a society or other partner) holds exclusive rights to this article under a publishing agreement with the author(s) or other rightsholder(s); author self-archiving of the accepted manuscript version of this article is solely governed by the terms of such publishing agreement and applicable law.